Research Article

Effect of Micropolar Fluid to Study the Characteristics of Squeeze Film Between Porous Curved Annular Plates

N. Chaithra*[1] (iD) and B. N. Hanumagowda[2] (iD)

[1] *Department of Mathematics, East Point College of Engineering and Technology, Bangalore 560049, Karnataka, India*

[2] *Department of Mathematics, School of Applied Sciences, REVA University, Bangalore 560064, Karnataka, India*

*Corresponding author: chaithra1590@gmail.com

Abstract. This study examines the effect of micropolar fluid lubricants on porous curved annular plates through a squeeze film lubrication approach. Squeeze film characteristics have been determined using a modified version of the Reynolds equation. Micropolar fluid has an improved impact on the squeeze film pressure, load bearing capacity, and squeeze film time compared to the Newtonian case, whereas porosity has an adverse effect on squeeze film characteristics.

Keywords. Micropolar fluids, Porous, Curved annular plates, Squeeze film

Mathematics Subject Classification (2020). 76D08, 76S05, 74DXX

1. Introduction

In recent years, due to its proposal in biophysical and hydrological issues, generally in petroleum and nuclear production, flow through the permeable medium has been assumed to be more important. Porous bearings are generally made from bronze or iron, which contains interconnecting pores. These bearings can work for a long time without using additional lubricants, and they can be used in many areas, where re-lubrication would be difficult. Thus, porous bearings are generally used in audiovisual equipment, coffee grinders, water pumps, etc. Because of these practical aspects, numerous theoretical studies have been carried out on porous bearings, including work by Prakash and Vij [11], who studied the porosity effect on inclined slider bearings. Morgan and Cameron [8] investigated the theory of hydrodynamic porous journal bearings. For two forms of geometry (annular and rectangular), Wu [14, 15] discussed the squeeze film output on the porous surface. In terms of the appearance of the micropolar fluid, Naduvinamani and Santosh [10] explored the nature of film lubrication between finitely porous journal bearings. It illustrates that the porous surface reduces film pressure, load and improves the journal centre velocity. Squeeze film technology is widely used in several fields, such as engines, turbomachinery devices, and skeletal joints. In general, squeeze film lubrication between approaching surfaces has been extensively studied by several investigators (see Gould [3], Gupta and Vora [4], and Hays [7]).

The analysis of micropolar fluid theory is very important due to its applications in industries. The inventive researcher Eringen [2] developed the theory of micropolar fluid. This includes randomly (or spherically), rigid particles suspended in a viscous medium in which fluid particle deformation is ignored. Many theories e.g., Agrawal and Bhatt [1], Naduvinamani Siddangouda [9], Siddangouda [12], Verma *et al*. [13], and Zaheeruddin and Isa [16] show that, load is greater when lubricated with a micropolar fluid, and the load is reduced due to the effect of porosity. In the presence of micropolar fluid, Hanumagouda *et al*. [5,6] investigated the squeeze film behavior in curved annular plates. But none of these authors have studied the addition of porosity to these curved annular bearings. Hence, in the appearance of micropolar fluid, this paper aims to examine the squeeze film behavior in porous curved annular plates.

2. Mathematical Formulation

Figure 1 displays the physical structure of porous curved annular plates, where the smooth surface of curved annular at the upper region and porous flat surfaces of lower approaching at the outer and inner radius are a and b respectively with a normal velocity V.

The exponential film shape h is defined as

$$h = h_m \exp\left(-\frac{\beta r^2}{a^2}\right), \quad b \le r \le a. \tag{2.1}$$

Here h_m represents the minimum film thickness, r is the radial axis and β is the parameter for the curvature. The governing equations are developed for this physical quantity, depending on balancing laws.
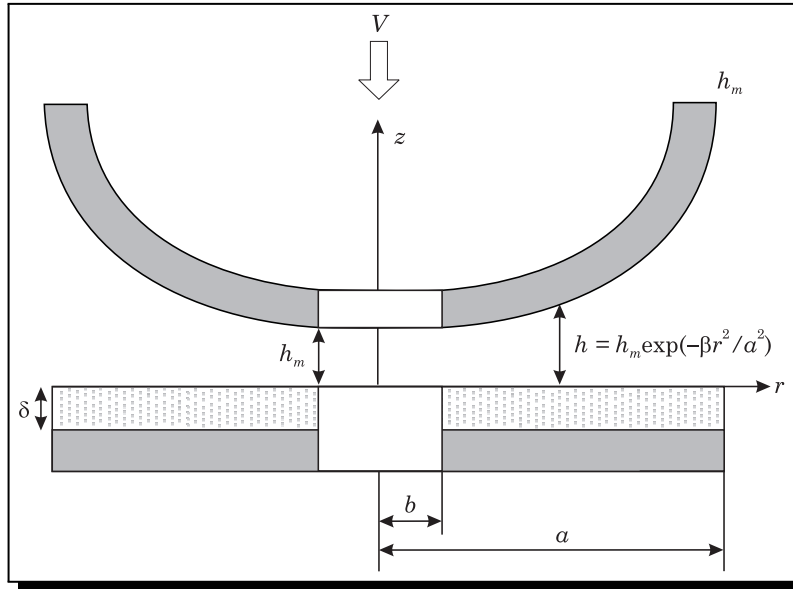
Figure 1. Physical geometry of squeeze film lubrication between porous curved annual plates

Conservation of linear momentum

$$\left(\mu + \frac{\chi}{2}\right)\frac{\partial^2 u}{\partial z^2} + \chi\frac{\partial w_1}{\partial z} = \frac{\partial p}{\partial r} \tag{2.2}$$

Conservation of angular momentum

$$\gamma\frac{\partial^2 w_1}{\partial z^2} - \chi\frac{\partial u}{\partial z} - 2\chi w_1 = 0 \tag{2.3}$$

Conservation of mass

$$\frac{1}{r}\frac{\partial}{\partial r}(ru) + \frac{\partial w}{\partial z} = 0 \tag{2.4}$$

The modified Darcy equations are given by

$$\left.\begin{array}{l} u^* = \dfrac{-k}{(\mu + \chi)}\dfrac{\partial p^*}{\partial r}, \\[3mm] w^* = \dfrac{-k}{(\mu + \chi)}\dfrac{\partial p^*}{\partial z}, \end{array}\right\} \tag{2.5}$$

where μ is the coefficient of viscosity, k is the porous surface permeability and p^* is the porous area pressure that obey the equation of Laplace

$$\frac{1}{r}\frac{\partial}{\partial r}\left(r\frac{\partial p^*}{\partial r}\right) + \frac{\partial^2 p^*}{\partial z^2} = 0. \tag{2.6}$$

With the help of the following boundary conditions, solve the equations (2.2) and (2.3).

At the smooth upper plate $z = h$:

$$u = 0, \quad w_1 = 0, \quad w = \frac{dh_m dt}{dt}. \tag{2.7}$$

At the porous lower plate $z = 0$:

$$u = 0, \quad w_1 = 0, \quad w = w^*, \tag{2.8}$$

gives,

$$
u = \frac{p'}{\mu}\left\{\frac{z^2}{2} - \frac{N^2 h}{m}\frac{(\cosh mz - 1)}{\sinh mh}\right\} + \frac{D_1}{(1-N^2)}\left[z - \frac{N^2}{m}\left\{\sinh mz - (\cosh mz - 1)\frac{(\cosh mh - 1)}{\sinh mh}\right\}\right]
$$

(2.9)

and

$$
w_1 = \frac{D_1}{2(1-N^2)}(\cosh mz - 1) + \frac{\sinh mz}{\sinh mh}\left\{\frac{hp'}{2\mu} - \frac{D_1}{2(1-N^2)}(\cosh mh - 1)\right\} - \frac{zp'}{2\mu},
$$

(2.10)

where

$$
m = \left\{\frac{4\mu\chi}{\gamma(2\mu+\chi)}\right\}^{\frac{1}{2}}, \quad N = \left(\frac{\chi}{2\mu+\chi}\right)^{\frac{1}{2}}, \quad D_1 = \frac{-(1-N^2)}{2}\left(\frac{hp'}{\mu}\right), \quad l = \left(\frac{\gamma}{4\mu}\right)^{\frac{1}{2}}.
$$

Integrate equation (2.6) with respect to z over the thickness of the porous layer δ and also using the boundary constraints $\frac{\partial p^*}{\partial z} = 0$ at $z = -\delta$ it can be obtained as

$$
\left(\frac{\partial p^*}{\partial z}\right)_{z=0} = -\int_{-\delta}^{0}\frac{1}{r}\frac{\partial}{\partial r}\left(r\frac{\partial p^*}{\partial r}\right)dz.
$$

(2.11)

Suppose porous layer thickness δ is too small and we get $p = p^*$ pressure continuity condition on the porous surface $z = 0$, we get

$$
\left(\frac{\partial p^*}{\partial z}\right)_{z=0} = -\frac{\delta}{r}\frac{\partial}{\partial r}\left(r\frac{\partial p}{\partial r}\right).
$$

(2.12)

Since the component of velocity w^* is given at the interface ($z = 0$)

$$
(w^*)_{z=0} = \frac{k\delta}{r(\mu+\chi)}\frac{\partial}{\partial r}\left(r\frac{\partial p}{\partial r}\right).
$$

(2.13)

Replacing the equation (2.9) in (2.4) and then integrate with z over h, using the boundary limits (2.7) and (2.8)

$$
\frac{1}{r}\frac{\partial}{\partial r}\left[\left\{f(N,l,h) + \frac{12\mu k\delta}{(\mu+\chi)}\right\}r\frac{\partial p}{\partial r}\right] = 12\mu\frac{dh_m}{dt},
$$

(2.14)

where $f(N,l,h) = h^3 + 12l^2 h - 6Nlh^2\coth\left(\frac{Nh}{2l}\right)$, and $m = \frac{N}{l}$.

Inserting the following dimensionless quantities

$$
r^* = \frac{r}{a}, \quad h^* = \frac{h}{h_{m0}} = h_m^*\exp(-\beta r^{*2}), \quad h_m^* = \frac{h_m}{h_{m0}}, \quad l^* = \frac{l}{h_{m0}}, \quad \delta^* = \frac{\delta}{h_{m0}},
$$

$$
P^* = \frac{ph_{m0}^3}{\mu a^2\left(\frac{-dh_m}{dt}\right)}, \quad \psi = \frac{k\delta}{h_{m0}^3}.
$$

Equation (2.14) becomes

$$
\frac{\partial}{\partial r^*}\left\{J^*(N,l^*,h^*,\psi)r^*\frac{\partial P^*}{\partial r^*}\right\} = -12r^*,
$$

(2.15)

where

$$
J^*(N,l^*,h^*,\psi) = f^*(N,l^*,h^*) + 12\psi\left(\frac{1-N^2}{1+N^2}\right).
$$

(2.16)

Integrating the equation (2.15), using the pressure boundary limits of porous region are

$$
P^* = 0 \quad \text{at} \quad r^* = \alpha = \frac{b}{a},
$$

(2.17)

$$
P^* = 0 \quad \text{at} \quad r^* = 1.
$$

(2.18)

Gives the dimensionless pressure as

$$P^* = \frac{6\{j_1(1)j_2(r^*) - j_2(1)j_1(r^*)\}}{j_2(1)}, \tag{2.19}$$

where

$$j_1(r^*) = \int_\alpha^{r^*} \frac{r^*}{J^*(N,l^*,h^*,\psi)}dr^*, \quad j_2(r^*) = \int_\alpha^{r^*} \frac{1}{r^* J^*(N,l^*,h^*,\psi)}dr^*,$$

$$j_1(1) = \int_\alpha^1 \frac{r^*}{J^*(N,l^*,h^*,\psi)}dr^* \quad \text{and} \quad j_2(1) = \int_\alpha^1 \frac{1}{r^* J^*(N,l^*,h^*,\psi)}dr^*.$$

In dimensionless form, the load bearing capacity W is represented as

$$W^* = \frac{Wh_{m0}^3}{2\pi\mu a^4 \left(\frac{-dh_m}{dt}\right)} = \frac{6\left\{j_1(1)\int_\alpha^1 j_2(r^*)r^*dr^* - j_2(1)\int_\alpha^1 j_1(r^*)r^*dr^*\right\}}{j_2(1)}. \tag{2.20}$$

The squeeze film time in dimensionless form is given by

$$T^* = \frac{Wh_{m0}^2}{\pi\mu a^4}t = 12\int_{h_m^*}^1 \left\{\frac{j_1(1)\int_\alpha^1 j_2(r^*)r^*dr^* - j_2(1)\int_\alpha^1 j_1(r^*)r^*dr^*}{j_2(1)}\right\}dh_m^*. \tag{2.21}$$

3. Results and Discussion

Several non-dimensional parameters are used to analyze the micropolar fluid lubrication characteristics of porous curved annular plates namely, coupling number N, permeability parameter ψ, couple stress parameter l^*, curvature parameter β and radius ratio α. For the numerical calculations, the following set of parametric values are used $l^* = 0.0, 0.2, 0.4$; $N = 0.0, 0.4, 0.8$; $\beta = -0.25, 0.0, 0.25$ and $\alpha = 0.0, 0.2, 0.4$ are chosen. The outcomes attained in this article reduces to the Newtonian case when $l^*, N \to 0$ and as the permeability parameter $\psi \to 0$ the results obtained in this paper reduce to the solid case which is discussed in the previous paper of Hanumagouda *et al.* [5] and these comparisons are represented in Table 1.

Table 1. Comparison of the squeeze film characteristics P^*, W^* and T^* between Hanumagowda *et al.* [5] and present analysis for various values of N, l^* and ψ with fixed $h_m^* = 0.5$, $\beta = 0.25$, $\alpha = 0.4$ and $r^* = 0.6$

| | | Hanumagowda *et al.* [5] | | Present analysis | | | |
| | | | | $\psi = 0$ | | $\psi = 0.01$ | |
	N	$l^* = 0$	$l^* = 0.2$	$l^* = 0$	$l^* = 0.2$	$l^* = 0$	$l^* = 0.2$
P^*	0	5.9338	5.9338	5.9338	5.9338	2.4788	2.4788
	0.4	5.9658	7.0466	5.9658	7.0466	2.9586	3.2037
	0.8	5.9985	15.1540	5.9985	15.1540	4.5734	8.4921
W^*	0	1.9235	1.9235	1.9235	1.9235	0.7628	0.7628
	0.4	1.9342	2.2845	1.9342	2.2845	0.9165	0.9890
	0.8	1.9451	4.9334	1.9451	4.9334	1.4507	2.6510
T^*	0	1.9235	1.9235	1.9235	1.9235	0.7628	0.7628
	0.4	1.9342	2.2845	1.9342	2.2845	0.9165	0.9890
	0.8	1.9451	4.9334	1.9451	4.9334	1.4507	2.6510

3.1 Squeeze Film Pressure

Figure 2 indicates the difference between pressure P^* versus r^* as a function of N and ψ. It displays that P^* is increased for raising the N values and also for decreasing ψ values. The variance of P^* along with r^* for various l^* and ψ values are represented in Figure 3. It shows that P^* is increased in order to increase the l^* values. The P^* deviation along with r^* is plotted in Figure 4 for different values of β and ψ. It displays that P^* increases for raising the β values.
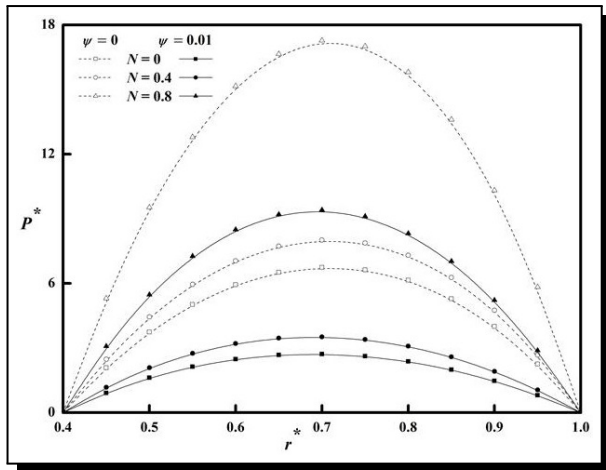
Figure 2. Plot of P^* versus r^* with $l^* = 0.2$, $h_m^* = 0.5$, $\beta = 0.25$ and $\alpha = 0.4$ for distinct values of ψ and N
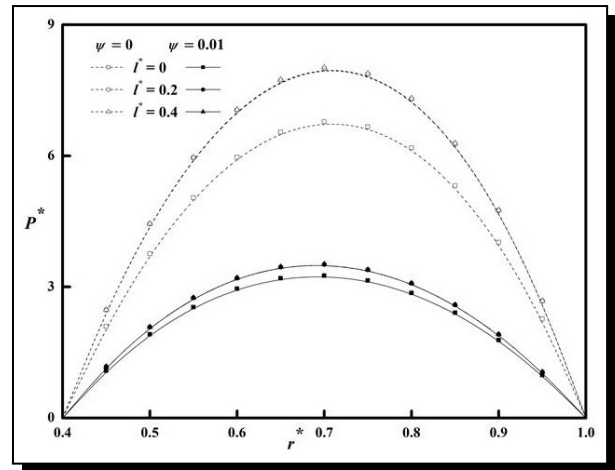
Figure 3. Plot of P^* versus r^* with $N = 0.4$, $h_m^* = 0.5$, $\beta = 0.25$ and $\alpha = 0.4$ for distinct values of ψ and l^*
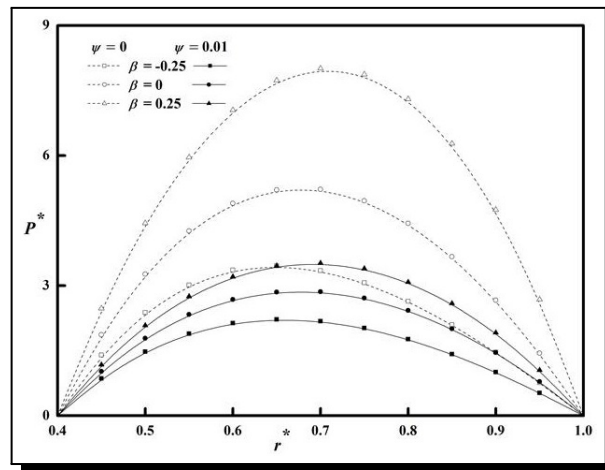
Figure 4. Plot of P^* versus r^* with $N = 0.4$, $l^* = 0.2$, $h_m^* = 0.5$ and $\alpha = 0.4$ for distinct values of ψ and β

3.2 Load Carrying Capacity

Figure 5 depicts the load profile W^* along β for specific N and ψ values. It is noted that W^* increases for raising N and decaying ψ values. Figure 6 represents the graph of W^* versus β for distinct l^* and ψ values. It is displayed that more load is obtained for the larger values

of couple stress parameter l^*. The graph of W^* against β is described in Figure 7 for various values of α and ψ. It is shows that load reduced by increasing the values of radius ratio α.
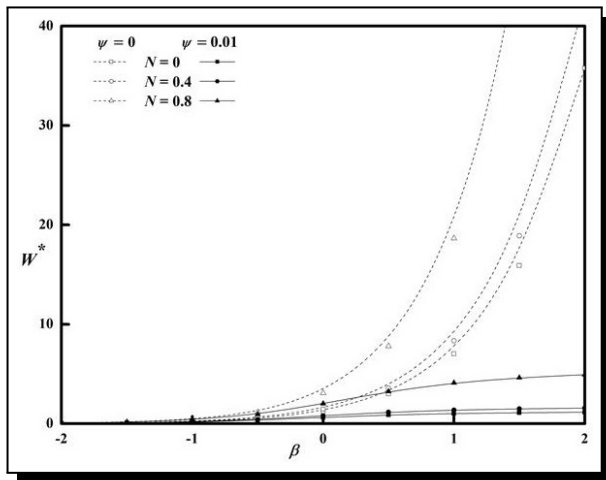

Figure 5. Plot of W^* versus β with $l^* = 0.2$, $h_m^* = 0.5$, and $\alpha = 0.4$ for distinct values of ψ and N
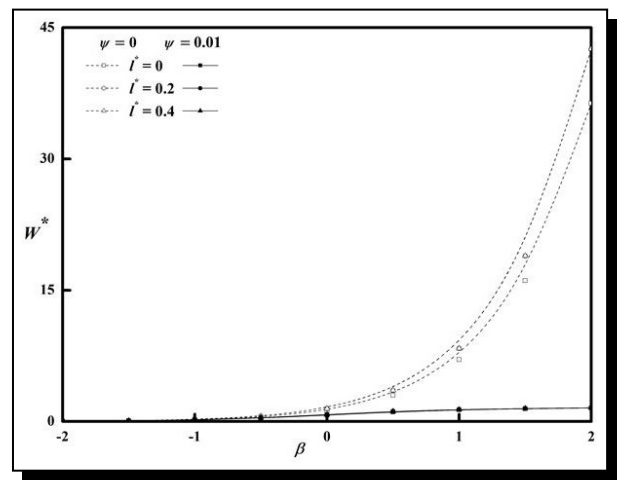

Figure 6. Plot of W^* versus β with $N = 0.4$, $h_m^* = 0.5$, and $\alpha = 0.4$ for distinct values of ψ and l^*
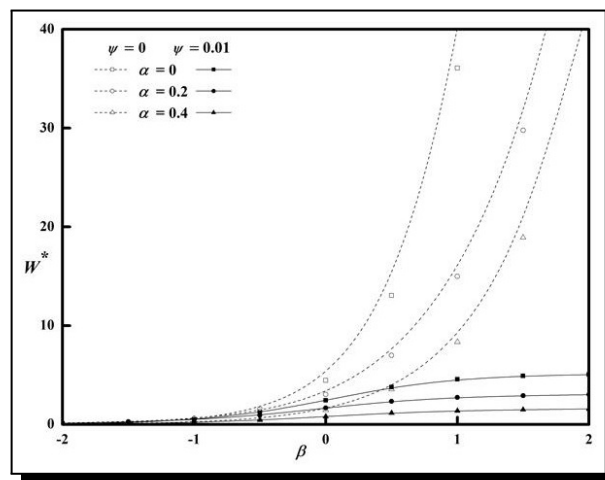

Figure 7. Plot of W^* versus β with $N = 0.4$, $h_m^* = 0.5$, and $l^* = 0.2$ for distinct values of ψ and α

3.3 Squeeze Film Time

Figure 8 shows the time profile T^* along with h_m^* as a function of N and ψ. It displays that T^* increases by raising the N and decreasing ψ values. Figure 9 represents the T^* variation along h_m^* for different l^* and ψ values. It is seen that T^* is increased for raising the l^* values. The deviation of T^* with h_m^* as a function of β and ψ is illustrated in Figure 10. It is observed that T^* raises for increasing the β values. Figure 11 represents the graph of T^* versus h_m^* for various values of α and ψ. It displays that time decays for increasing α values.
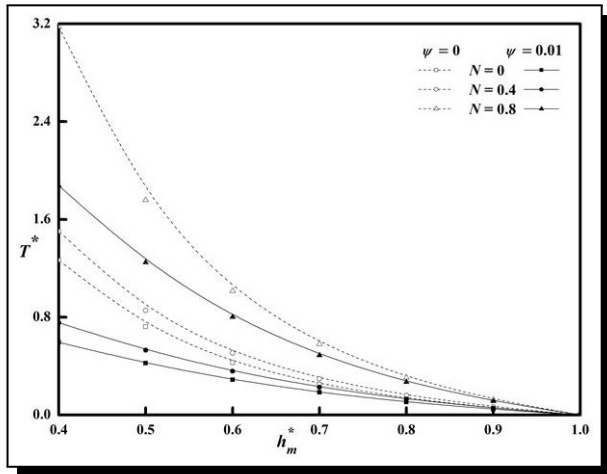
Figure 8. Plot of T^* versus h_m^* with $l^* = 0.2$, $\alpha = 0.4$ and $\beta = 0.25$ for distinct values of ψ and N
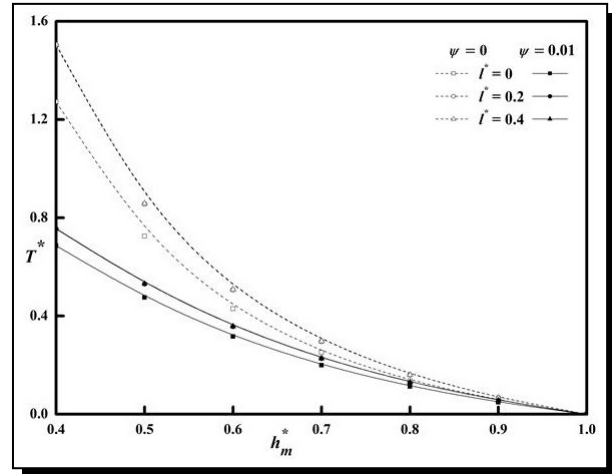

Figure 9. Plot of T^* versus h_m^* with $N = 0.4$, $\alpha = 0.4$ and $\beta = 0.25$ for distinct values of ψ and l^*
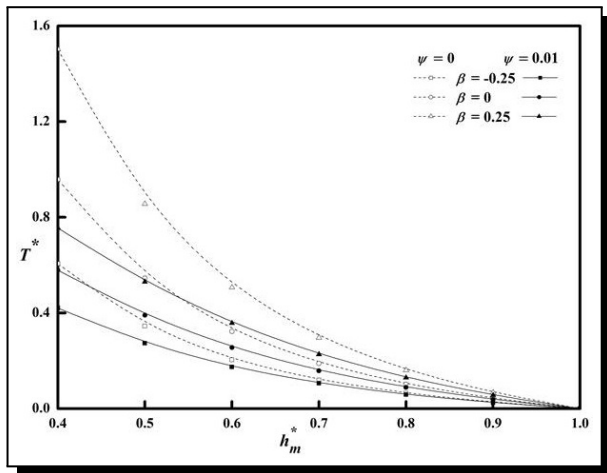

Figure 10. Plot of T^* versus h_m^* with $N = 0.4$, $l^* = 0.2$, and $\alpha = 0.4$ and for distinct values of ψ and β
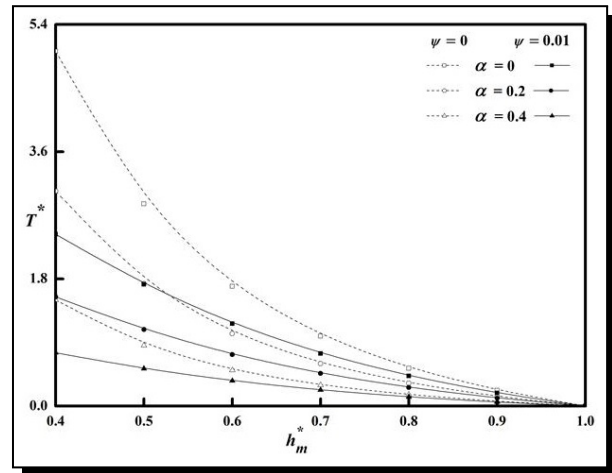

Figure 11. Plot of T^* versus h_m^* with $N = 0.4$, $l^* = 0.2$, and $\beta = 0.25$ and for distinct values of ψ and α

4. Conclusions

We examine the micropolar fluid impact on the squeeze film lubrication among porous curved annular plates. The conclusions are drawn as follows from the numerical computation of the outcomes.

  (i) Due to the impact of micropolar fluid, pressure, load and film time significantly increases.
 (ii) The presence of porous surface is to reduce the pressure, load-carrying capacity and squeeze film time.
(iii) The load bearing capacity and response time decreases with the rising radius ratio values.

Nomenclature

a	Outer radius of the plate
b	Inner radius of the plate
h	Film thickness
h_m	Minimum film thickness
h_{m0}	Minimum film thickness under steady state
h_m^*	Non-dimensional film thickness
k	Permeability of the porous matrix
l	Couple stress parameter $(\gamma/4\mu)^{\frac{1}{2}}$
l^*	Non-dimensional couple stress parameter (l/h_{m0})
N	Coupling number $\left(\frac{\chi}{2\mu+\chi}\right)^{\frac{1}{2}}$
p	Pressure in the film region
P^*	Non-dimensional fluid film pressure
r, z	Radial and axial coordinates
r^*	Non-dimensional radial coordinate (r/a)
t	Time of approach
T^*	Non-dimensional time of approach
u, w	Velocity components in r and z directions
u^*, w^*	Modified Darcy velocity components in r and z directions respectively
W	Load carrying capacity
W^*	Non-dimensional load carrying capacity

Greek Symbols

β	Curvature parameter
μ	Lubricant viscosity
δ	Porous layer thickness
α	Radius ratio
χ	Spin viscosity
γ	Viscosity coefficient for micropolar fluids
ψ	Permeability parameter $(k\delta/h_{m0}^3)$

Competing Interests

The authors declare that they have no competing interests.

Authors' Contributions

All the authors contributed significantly in writing this article. The authors read and approved the final manuscript.

References

[1] V. K. Agrawal and S. B. Bhatt, Porous pivoted slider bearings lubricated with a micropolar fluid, *Wear* **61**(1) (1980), 1 – 8, DOI: 10.1016/0043-1648(80)90106-4.

[2] A. C. Eringen, Theory of micropolar fluids, *Journal of Mathematics and Mechanics* **16**(1) (1966), 1 – 18, URL: http://www.iumj.indiana.edu/IUMJ/ABS/1967/16001.

[3] P. Gould, Parallel surface squeeze films: the effect of the variation of viscosity with temperature and pressure, *ASME Journal of Tribology* **89**(3) (1967), 375 – 380, DOI: 10.1115/1.3616998.

[4] J. L. Gupta and K. H. Vora, Analysis of squeeze films between curved annular plates, *ASME Journal of Tribology* **102**(1) (1980), 48 – 50, DOI: 10.1115/1.3251436.

[5] B. N. Hanumagowda, N. Chaithra and A. Salma, Effect of micropolar fluids on squeeze film lubrication between curved annular plates, *Journal of Physics: Conference Series* **1000** (2018), 1 – 8, DOI: 10.1088/1742-6596/1000/1/012088.

[6] B. N. Hanumagowda, N. Chaithra, H. S. Doreswamy and A. Salma, Combined effect of surface roughness and micropolar fluids on squeeze film characteristics between rough flat plate and curved annular plates, *Malaya Journal of Matematik* **8**(2) (2020), 570 – 575, DOI: 10.26637/MJM0802/0043.

[7] D. F. Hays, Squeeze films for rectangular plates, *ASME Journal of Fluids Engineering* **88**(2) (1963), 243 – 246, DOI: 10.1115/1.3656568.

[8] V. T. Morgan and A. Cameron, Mechanism of lubrication in porous metal bearings, in: *Proceedings of the Conference on Lubrication and Wear* (1st-3rd October 1957, London), **89** (1957), 151 – 157.

[9] N. B. Naduvinamani and A. Siddangouda, Porous inclined stepped composite bearings with micropolar fluid, *Tribology – Materials, Surfaces & Interfaces* **1**(4) (2007), 224 – 232, DOI: 10.1179/175158408X317109.

[10] N. B. Naduvinamani and S. Santosh, Micropolar fluid squeeze film lubrication of finite porous journal bearing, *Tribology International* **44**(4) (2011), 409 – 416, DOI: 10.1016/j.triboint.2010.11.019.

[11] J. Prakash and S. K. Vij, Load capacity and time-height relations for squeeze films between porous plates, *Wear* **24**(3) (1973), 309 – 322, DOI: 10.1016/0043-1648(73)90161-0.

[12] A. Siddangouda, Squeezing film characteristics for micropolar fluid between porous parallel stepped plates, *Tribology in Industry* **37**(1) (2015), 97 – 106, URL: http://www.tribology.fink.rs/journals/2015/2015-1/13.pdf.

[13] P. D. S. Verma, V. K. Agrawal and S. B. Bhatt, Porous inclined slider bearing lubricated with micropolar fluid, *Wear* **53**(1) (1979), 101 – 106, DOI: 10.1016/0043-1648(79)90221-7.

[14] H. Wu, An analysis of the squeeze film between porous rectangular plates, *ASME Journal of Tribology* **94**(1) (1972), 64 – 68, DOI: 10.1115/1.3451637.

[15] H. Wu, Squeeze-film behavior for porous annular disks, *ASME Journal of Tribology* **92** (4) (1970), 593 – 596, DOI: 10.1115/1.3451481.

[16] Kh. Zaheeruddin and M. Isa, Characteristics of a micropolar lubricant in a squeeze film porous spherical bearing, *Wear* **51**(1) (1978), 1 – 10, DOI: 10.1016/0043-1648(78)90049-2.